Journal of Innovations in Engineering Education
JIEE 2026, Vol. 9, Issue 1.

https://doi.org/10.3126/jiee.v9i1.90556

THAPATHALI CAMPUS
Institute of Engineering
Tribhuvan University

# Aerodynamic performance of double-wedge airfoils in supersonic flow at Mach 2

Bibek Dhungana[a], Lochan Kendra Devkota[a,*] and Pratik Adhikari[a]

[a]*Department of Automobile and Mechanical Engineering, Thapathali Campus, Institute of Engineering, Tribhuvan University*

ARTICLE INFO

*Article history*:

Received 4 February 2026
Revised in 1 April 2026
Accepted 4 April 2026

*Keywords:*

Double-wedge airfoil
Supersonic aerodynamics
RANS
Shock expansion theory

Abstract

A systematic computational investigation is presented to evaluate the aerodynamic performance of symmetric double-wedge airfoils operating in supersonic flow at Mach 2. Using Reynolds-Averaged Navier–Stokes (RANS) simulations with the standard $k-\epsilon$. turbulence model, the effects of thickness-to-chord ratio (t/c = 0.1-0.5) and angle of attack ($5°\leq \alpha \leq 15°$) on lift, drag, aerodynamic efficiency, and surface pressure distribution are examined. The numerical framework is validated against published experimental data at comparable Mach numbers, showing good agreement over a wide range of angles of attack. Results indicate that lift increases quasi-linearly with angle of attack for all configurations, while drag exhibits a strong sensitivity to both angle of attack and airfoil thickness. Thinner airfoils consistently demonstrate superior lift-to-drag ratios, particularly at moderate angles of attack ($\alpha \leq 5°$) whereas thicker sections incur significant drag penalties due to stronger shock-induced pressure gradients. Pressure coefficient distributions reveal a characteristic compression-expansion behavior along the chord, with stagnation pressure at the leading edge increasing markedly with thickness. The findings provide design-relevant insights into the aerodynamic trade-offs associated with thickness variation in double-wedge airfoils for supersonic cruise applications.



## 1. Introduction

The pursuit of efficient supersonic flight continues to motivate extensive research into airfoil geometries capable of managing strong compressibility effects, shock waves, and elevated wave drag. At flight speeds exceeding the speed of sound, aerodynamic performance is dominated by shock-expansion processes that significantly alter pressure, temperature, and velocity fields around lifting surfaces [1]. Conventional cambered airfoils, optimized for subsonic and transonic regimes, often suffer severe drag penalties and flow separation when operated in the supersonic domain. Consequently, airfoil configurations featuring sharp leading edges and planar surfaces have emerged as practical alternatives for high-speed applications[2]. Among these configurations, the symmetric double-wedge airfoil represents a canonical geometry in supersonic aerodynamics. Its simplicity allows for predictable shock formation at the leading edge and expansion processes downstream, making it particularly attractive for theoretical analysis and numerical investigation. Double-wedge sections have been employed in a variety of high-speed vehicles, including supersonic transports, missiles, and re-entry bodies, where robustness and shock control are critical design considerations [3], [4].

Previous experimental and numerical studies have demonstrated that the aerodynamic characteristics of double-wedge airfoils are strongly influenced by geometric parameters such as wedge angle, thickness-to-chord ratio, and angle of attack. Variations in these parameters affect not only lift and drag but also shock strength, pressure distribution, and overall aerodynamic efficiency. While several investigations have addressed isolated aspects of double-wedge performance, a systematic assessment of thickness effects over a broad range of angles of attack at a fixed supersonic Mach number remains limited in the open literature [5]. The

*Corresponding author:
lochan.devkota@tcioe.edu.np (L.K. Devkota)

present study aims to address this gap by providing a detailed numerical evaluation of the aerodynamic performance of symmetric double-wedge airfoils at Mach 2. Emphasis is placed on quantifying how thickness variation influences lift, drag, lift-to-drag ratio, and surface pressure characteristics across a wide angle-of-attack range. By focusing on performance metrics relevant to preliminary aerodynamic design, this work seeks to establish clear trends and trade-offs that can inform the selection of double-wedge airfoil geometries for sustained supersonic cruise.

### 1.1. Research problem and motivation

Despite the extensive use of double-wedge airfoils in supersonic applications, their aerodynamic performance remains highly sensitive to geometric parameters such as thickness-to-chord ratio and operating angle of attack. Increasing airfoil thickness can enhance structural integrity and volume availability; however, it also intensifies shock strength and wave drag, potentially degrading overall aerodynamic efficiency. Conversely, thinner configurations may offer improved lift-to-drag ratios but at the cost of reduced structural margins.

Existing studies often focus on isolated geometries or narrow operating conditions, making it difficult to extract generalized design guidelines regarding thickness effects at a given supersonic Mach number. Furthermore, while shock behavior has been widely studied from a theoretical standpoint, fewer investigations emphasize performance-oriented metrics- such as lift, drag, and aerodynamic efficiency- across a systematic range of thickness ratios and angles of attack under consistent flow conditions.

The research problem addressed in this study is therefore the lack of a comprehensive, performance-focused assessment of how thickness variation influences the aerodynamic characteristics of symmetric double-wedge airfoils operating at a fixed supersonic Mach number. Addressing this gap is essential for preliminary aerodynamic design, where rapid evaluation of geometric trade-offs is required.

### 1.2. Literature review

The quest for supersonic flight began in earnest in the early 20th century, driven by the desire to achieve higher speeds and improve aircraft performance. Theoretical groundwork was laid by Ernst Mach, whose studies on shock waves and compressible flow provided a foundational understanding of the phenomena associated with speeds exceeding the speed of sound [6]. The evolution of airfoil designs has been pivotal in advancing supersonic flight. Early supersonic aircraft utilized simple, thin straight-wing designs, which were found to be inefficient due to high drag and limited maneuverability. The advent of swept-wing designs, such as those used in the North American F-86 Sabre, provided better performance by delaying shock wave formation and reducing drag [7]. Linear theory, also known as linearized supersonic flow theory, provides a simplified method for analysing supersonic flows around slender bodies or airfoils at small angles of attack. The essential premise is that the object's presence will result in negligible perturbations in the flow field, enabling the linearization of the governing equations [8]. By assuming slight velocity disturbances, the potential flow equation is linearized in linear theory [9]. The velocity potential $\phi$ is used to describe the flow field, where the perturbation velocity components ($u'$,$v'$,$w'$) are the derivatives of $\phi$:

$$u' = \frac{\partial \phi}{\partial x}, \quad v' = \frac{\partial \phi}{\partial y} \tag{1}$$

Then the linearized potential equation for a supersonic flow becomes:

$$\frac{\partial^2 \phi}{\partial x^2} - \frac{1}{M^2}\frac{\partial^2 \phi}{\partial y^2} + \frac{\partial^2 \phi}{\partial z^2} = 0 \tag{2}$$

Shock expansion theory is one of the best ways to think about shock and fan expansion in supersonic flow. This theory is especially useful for analysing the flow of airfoils and other devices with sharp edges and corners, such as wings. When a supersonic flow encounters changes in geometry, such as edges or corners, a weak shock is created [10]. In case of shock, flow characteristics (pressure, temperature, velocity) change almost instantly. When the supersonic flow meets the lobe, a fan expansion (also known as Prandtl-Meyer expansion) occurs. The rapid water flow through the fan expands, causing pressure and temperature to decrease as Mach number increases [11].

$$\begin{aligned} \rho_1 u_1 &= \rho_2 u_2\text{: Mass Conservation} \\ P_1 + \rho_1 u_1^2 &= P_2 + \rho_2 u_2^2\text{: Momentum Conservation} \\ h_1 + \frac{u_1^2}{2} &= h_2 + \frac{u_2^2}{2}\text{: Energy Conservation} \end{aligned} \tag{3}$$

Further these expressions can be combined to determine the fluid flow parameters before and after the shock region as shown below:

$$\begin{aligned}
\frac{P_2}{P_1} &= 1 + \frac{2\gamma}{\gamma+1}(M_1^2 - 1) \\
\frac{\rho_2}{\rho_1} &= \frac{(\gamma+1)M_1^2}{(\gamma-1)M_1^2 + 2} \\
\frac{T_2}{T_1} &= \left[\frac{2\gamma M_1^2 - (\gamma-1)}{(\gamma+1)^2}\right] \\
&\times \left[\frac{(\gamma-1)M_1^2 + 2}{\gamma+1}\right]
\end{aligned} \tag{4}$$

In the above equations, subscript 1 and 2 denotes the respective flow properties upstream and downstream of the shock. Shock expansion theory combines the effects of weak shocks and expanding fans to analyze flows with complex geometries. For example, in a two-wedge airfoil, the leading edge creates a shock wave while the trailing edge creates an expansion fan. Using the shock relationship and the Prandtl-Meyer function, the flow characteristics around the entire airfoil can be determined [12].

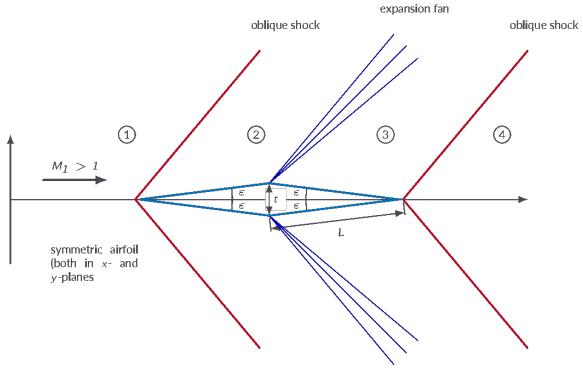


Figure 1: Shock expansion theory illustration [13],[14]

The double-edged airfoil has a symmetrical shape with two lines intersecting at the leading edge and diverging again at the trailing edge [15]. The aerodynamic performance of a two-wedge airfoil in supersonic flow is determined only by the interaction of shock waves and expansion fans produced by the leading edge and trailing edge, respectively [13]. When supersonic flow meets the edge of a double-edged airfoil, a shock wave is created. This oblique shock wave increases pressure and temperature while decreasing the speed of airflow. The shock wave angle ($\beta$) can be determined using the oblique shock relations:

$$\tan(\beta) = \frac{2\cot\theta_1(M_1^2\sin^2\theta_1 - 1)}{(M_1^2(\gamma + \cos 2\theta_1) + 2} \tag{5}$$

## 2. Numerical methodology

### 2.1. Airfoil geometry and computational domain

The study investigates a series of double-wedge (diamond-shaped) airfoils with thickness-to-chord ($\frac{t}{c}$) ratios ranging from 0.1 to 0.5. All models utilized a constant unit chord length. General applications of double wedge airfoil can be restricted between airfoil thickness and aerodynamic limitations as shown in figure 1. Thinner airfoil has structural limitations and thicker ones has disadvantages on aerodynamic performances. Analysis of airfoil with range of ($t/c$) values are associated to identify the tradeoffs for the real-world application.

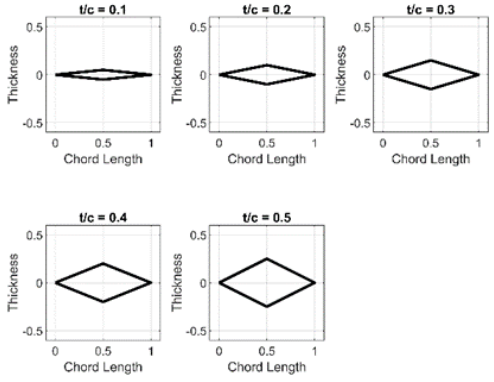


Figure 2: Airfoil geometry

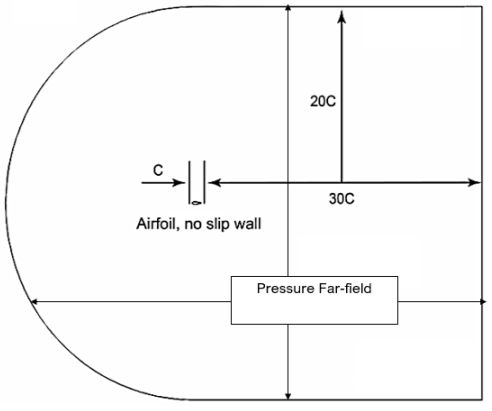


Figure 3: Computational domain showing C-type grid and boundary condition

To simulate an unconfined supersonic environment, a C-

type computational domain was established, extending 12.5C upstream and 30C downstream from the trailing edge to prevent boundary-induced flow interference [14]. Airfoil rotation and flow behavior capture at different angles of attack were configured using a parametric rotation approach which can be configured in ANSYS project browser. ANSYS Fluent models a free-stream condition at infinity using pressure far-field conditions, wherein static circumstances and the free-stream Mach number are provided. Since the pressure far-field boundary condition determines the flow variables at the boundaries using characteristic information (Riemann invariants), it is frequently referred to as a characteristic boundary condition. The pressure far-field boundary condition is only relevant when the ideal-gas law is used to compute the density.

## 2.2. Mesh generation and independence

The domain was discretized using a structured C-type mesh composed of quadrilateral elements. To resolve the complex shock-boundary layer interactions and viscous effects near the airfoil, a high-density grid was clustered in the immediate vicinity of the solid surfaces. A mesh independence study was conducted by evaluating the sensitivity of the drag coefficient $C_D$ to the element count, ensuring that the final numerical results were grid-independent. As seen in the figure 4 and 5, number of mesh over 82,000 elements for Double-Wedge airfoil are able to generate precise results with minimal deviation within 0.1%. The central segmented section has an element size of 0.5mm and the rest of the surface has 2mm element. In the domain the Jacobean ratio of elements was kept near 1, skewness was limited to within 0.25, average aspect ratio of the cells were 1.2 and orthogonality quality is close to 0.

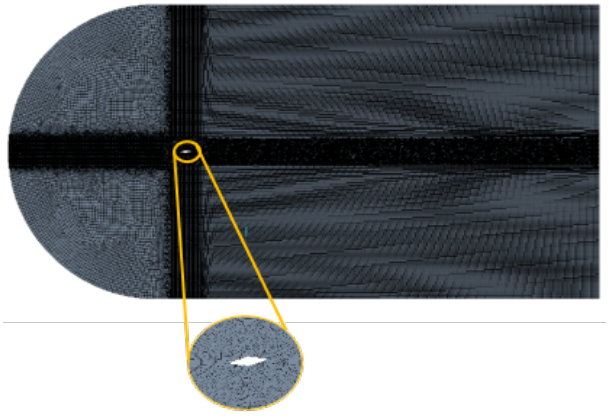

Figure 4: Mesh of the airfoil illustrating mesh elements and clustering

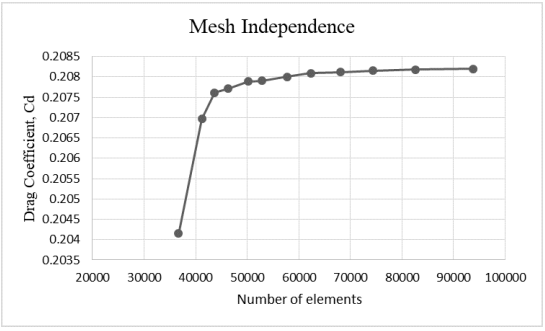


Figure 5: Mesh independence plot validating drag coeff with number of elements

## 2.3. Solver and boundary conditions

Numerical simulations were performed using the commercial CFD package ANSYS Fluent, employing a Reynolds-Averaged Navier-Stokes (RANS) solver. The working fluid air is assumed to be an ideal gas model, which means it follows the ideal gas law relating to pressure, temperature and density. The Sutherland viscosity model is used to describe the variation of dynamic viscosity ($\mu$) of air with temperature. It is based on the following relation:

$$\mu = \mu_{ref} \left( \frac{T}{T_{ref}} \right)^{3/2} \frac{T_{ref} + S}{T + S} \tag{6}$$

The Sutherland viscosity model [16] allows for more accurate representation of air viscosity over a wider range of temperatures compared to constant viscosity models. Turbulence was captured using the $k-\epsilon$ model[17], which utilized optimized empirical constants to enhance accuracy in the supersonic regime. The airfoil surface was defined as a "no-slip" wall, while the outer boundaries were set as "pressure far-field" to accurately model free-stream Mach number conditions at infinity.

## 2.4. Turbulence modeling

The standard $k-\epsilon$ turbulence model is one of the most widely used models for simulating turbulent flows in CFD It is a two-equation model that solves for two additional transport equations: one for the turbulent kinetic energy ($k$) and another for the turbulent dissipation rate ($\epsilon$). The k-epsilon turbulence model adds two additional transport equations for turbulent quantities: Turbulent Kinetic Energy ($k$) Equation:

$$\frac{\partial(\rho k)}{\partial t} + \nabla \cdot (\rho \mathbf{u} k) = \nabla \cdot \left( \mu + \frac{\mu_t}{\sigma_k} \right) \nabla k + P_k - \rho\epsilon \tag{7}$$

Turbulent Dissipation rate ($\epsilon$ Equation:

$$\frac{\partial(\rho\epsilon)}{\partial t}+\nabla\cdot(\rho\mathbf{u}\epsilon) = \nabla\cdot\left[\left(\mu+\frac{\mu_t}{\sigma_\epsilon}\right)\nabla\epsilon\right]+C_{\epsilon 1}\frac{\epsilon}{k}P_k-C_{\epsilon 2}\rho\frac{\epsilon^2}{k} \tag{8}$$

In the present study, the standard $k-\epsilon$ turbulence model was employed with the conventional model constants $C_\mu$=0.01, $C_{\epsilon 1}$=1.4 and $C_{\epsilon 2}$=1.92. Minor adjustments to selected constants were performed where necessary to improve agreement with experimental data and established theoretical solutions. Near-wall treatment was handled using an improved wall function approach to ensure accurate prediction of flow variables in the viscous sublayer and logarithmic regions without fully resolving the boundary layer.

### 2.5. Numerical schemes and validation

For numerical stability, a pressure-based implicit formulation was adopted [17]. The Roe Finite Difference Scheme (Roe-FDS) was utilized for spatial discretization to effectively resolve shock waves and discontinuities within the flow field. Gradient calculations for pressure and velocity were performed using the least squares cell-based method. A least squares cell-based method is used to compute gradients of scalar values like pressure, velocity, and temperature[18]. By reducing the squared disparities between values of nearby cells, this approach improves the accuracy of gradient calculations. The flow equations' convective terms are solved using the second order upwind technique. By adding data from nearby cells, this technique improves accuracy while retaining the advantages of upwind differencing, producing a more accurate depiction of the convective flow. The first order upwind technique is used for the transmission of turbulent kinetic energy ($k$). Stable and reliable findings are guaranteed by this method of calculating the transport, which takes the upstream value at the cell face into account. Likewise, in the $k-\epsilon$ turbulence model, the turbulent dissipation rate ($\epsilon$) is spatially discretized using the first order upwind approach. The requirement for numerical solution stability at a suitable level of precision is the driving force behind this decision. The computational model was validated by comparing the simulated lift coefficients $C_L$ against established experimental and theoretical data at Mach 1.86 [19], [20], demonstrating high fidelity in predicting aerodynamic performance with deviations of less than $\pm$2%.

## 3. Results

The supersonic flow properties such as Mach number, pressure contours and other results, namely lift and drag coefficient, pressure coefficient are extracted from CFD post. Mach number and pressure contours for fixed

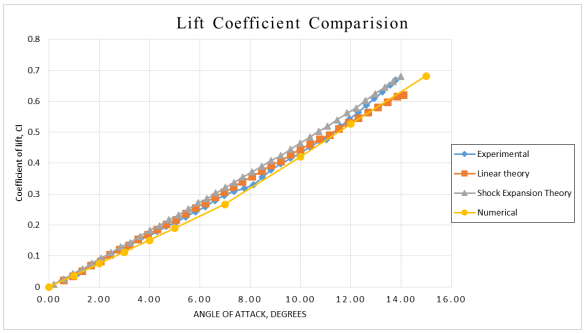


Figure 6: Comparison between lift coefficient against angle of attack at M=1.86

Mach of 2 are shown below for angle of attacking ranging $-5$-, 0-, 5- and 10-. However, the overall simulation data acquired have the angle of attack ranging $-5$- to 15-

### 3.1. Flow field characteristics

The flow field around the double-wedge airfoils at Mach 2 is characterized by a combination of oblique shock waves, expansion fans, and regions of accelerated supersonic flow. The sharp leading edge of the airfoil generates a compression wave that evolves into an oblique shock, followed by an expansion process downstream of the mid-chord where the surface inclination changes. The strength and spatial extent of these features are strongly influenced by both the airfoil thickness-to-chord ratio and the angle of attack. Representative Mach number contours for selected thickness ratios and angles of attack are shown in Figure 7-11. At zero angle of attack, all configurations exhibit symmetric flow patterns about the chord line. Thinner airfoils produce weaker leading-edge shocks with smaller pressure jumps, while thicker airfoils generate stronger compression waves due to the larger effective wedge angle. As thickness increases, the shock becomes more pronounced and the region of reduced Mach number downstream of the shock expands, indicating increased shock-induced losses.

With increasing angle of attack, the flow field becomes asymmetric, and the shock strength on the windward surface increases significantly. For moderate angles of attack ($\alpha \leq 5$-), the shock remains attached to the leading edge for thinner configurations, and the overall flow structure remains orderly. In contrast, thicker airfoils exhibit stronger shock systems and larger regions of compressed flow even at relatively small angles of attack, highlighting their increased sensitivity to incidence in supersonic conditions. At higher angles of attack, the interaction between shock waves and the boundary layer becomes more prominent, particularly

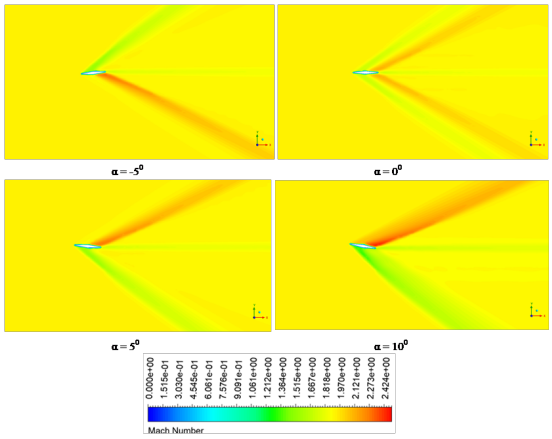


Figure 7: Mach number contour (t/c=0.1)

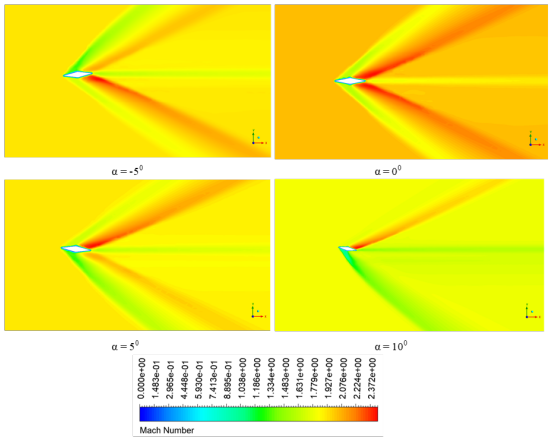


Figure 8: Mach number contour (t/c=0.2)

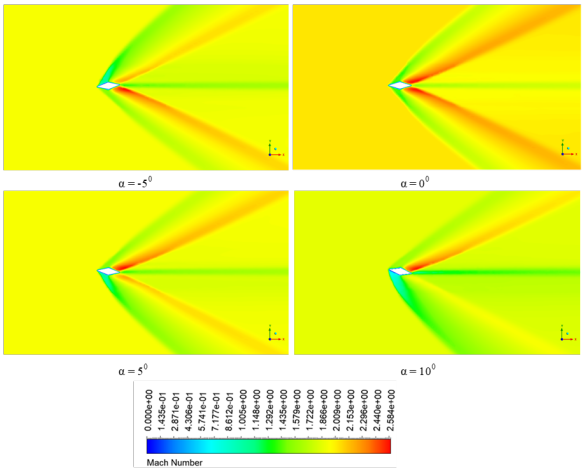


Figure 9: Mach number contour (t/c=0.3)

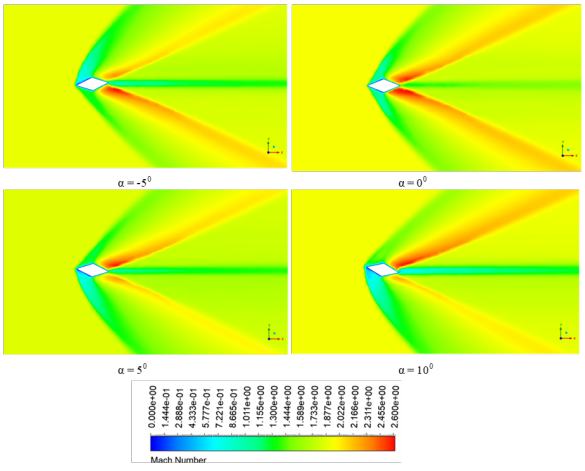


Figure 10: Mach number contour (t/c=0.4)

for larger thickness ratios. The intensified compression on the windward surface leads to higher local pressure gradients and a corresponding increase in wave drag. Although detailed shock detachment mechanisms are not the focus of the present performance-oriented study, the observed flow features provide qualitative insight into the aerodynamic trends discussed in subsequent sections. Overall, the Mach contour visualizations illustrate that increasing airfoil thickness leads to stronger shock systems and larger regions of decelerated flow, which directly influence the aerodynamic forces acting on the airfoil. These flow characteristics form the physical basis for the lift, drag, and efficiency trends analyzed in the following subsections.

### 3.2. Lift characteristics

The variation of lift coefficient with angle of attack for the investigated double-wedge airfoil configurations is presented in Figure 11 for thickness-to-chord ratios ranging from t/c = 0.1 to 0.5. For all configurations, the lift coefficient exhibits a predominantly linear increase with angle of attack over the investigated range, which is consistent with classical supersonic airfoil theory for sharp-edged profiles. At negative angles of attack, the lift coefficients are correspondingly negative and symmetric in magnitude, reflecting the geometric symmetry of the airfoil. As the angle of attack increases from 5° to positive values, lift generation is governed primarily by the pressure difference between the windward and leeward surfaces induced by shock compression and expansion effects. The linearity of the lift curve at lower and moderate angles of attack indicates that the flow remains largely attached and dominated by inviscid compressibility effects. Airfoil thickness has a noticeable influence on lift magnitude at a given angle of attack. Thicker airfoils generally produce slightly higher lift coefficients at the same angle of attack compared to thinner configurations. This behavior can be attributed to the

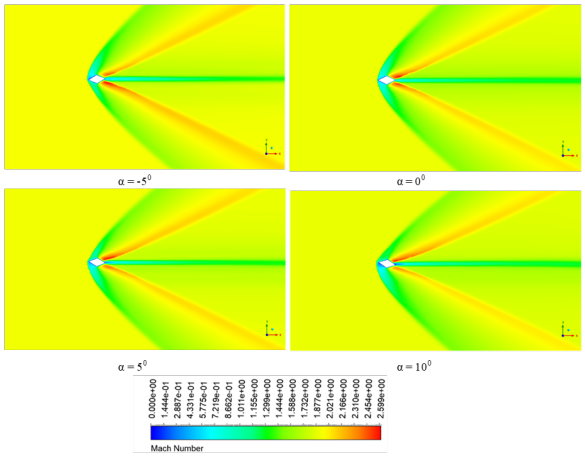


Figure 11: Mach number contour (t/c=0.5)

increased effective flow deflection and stronger pressure rise on the windward surface associated with larger wedge angles. However, the differences in lift between thickness ratios are relatively modest when compared to the corresponding variations in drag, as discussed in the following subsection. At higher angles of attack ($\alpha \geq 10$-), deviations from perfect linearity begin to appear, particularly for the thicker airfoil configurations. These deviations are associated with increasingly strong shock–boundary layer interactions and elevated pressure gradients on the windward surface. Although no abrupt loss of lift is observed within the examined range, the rate of lift increase with angle of attack diminishes slightly for the thickest configurations, indicating the onset of aerodynamic inefficiencies at higher incidence. Overall, the lift results demonstrate that double-wedge airfoils retain predictable and nearly linear lift behavior at Mach 2 over a wide range of angles of attack. While increasing thickness offers marginal lift benefits, these gains must be evaluated in conjunction with the significant drag penalties incurred by thicker airfoils, which are examined in detail in the next section.

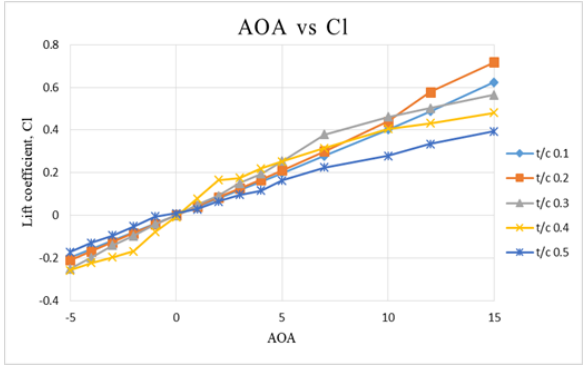


Figure 12: AOA vs lift coeff. at different t/c ratios

## 3.3. Drag characteristics

The variation of drag coefficient with angle of attack for the investigated double-wedge airfoil configurations is shown in Figure 13 for thickness-to-chord ratios ranging from $\frac{t}{c} = 0.1$ to 0.5. In contrast to lift, which exhibits a relatively uniform linear trend, drag is highly sensitive to both airfoil thickness and angle of attack in the supersonic regime. At zero angle of attack, the drag coefficient increases systematically with increasing thickness. Thinner airfoils exhibit the lowest drag values due to weaker leading-edge shocks and reduced wave drag, whereas thicker configurations generate stronger compression waves that result in higher pressure drag even at zero incidence. This behavior underscores the dominant role of wave drag in determining the aerodynamic performance of supersonic airfoils with finite thickness. As the angle of attack increases, drag rises nonlinearly for all configurations. For moderate angles of attack ($\alpha \leq 5$-, the increase in drag remains relatively gradual, particularly for thinner airfoils. However, beyond this range, the rate of drag increase becomes significantly steeper, especially for airfoils with larger thickness ratios. This trend is associated with intensified shock strength on the windward surface and increased pressure gradients that amplify wave drag contributions. The influence of thickness on drag becomes increasingly pronounced at higher angles of attack. For $t/c0.4$, the drag coefficient increases sharply with angle of attack, reflecting the combined effects of strong shock compression and enhanced viscous losses. These configurations experience substantially higher drag penalties compared to thinner airfoils operating under identical flow conditions, highlighting their reduced aerodynamic efficiency in supersonic flight. Overall, the drag results clearly demonstrate that airfoil thickness is a critical parameter governing aerodynamic performance at Mach 2. While thicker airfoils may offer structural or volumetric advantages, they incur significant drag penalties that can outweigh their modest lift benefits. These findings emphasize the importance of minimizing thickness in the preliminary design of double-wedge airfoils intended for efficient supersonic operation. .

## 3.4. Aerodynamic efficiency

The aerodynamic efficiency of the double-wedge airfoils is evaluated using the lift-to-drag ratio ($C_l/C_d$ ), which is plotted as a function of angle of attack for all thickness-to-chord ratios in Figure 14. This metric provides a direct measure of the trade-off between lift generation and drag penalties in supersonic flight and is therefore of primary interest for preliminary aerodynamic design.

For all configurations, the lift-to-drag ratio increases with angle of attack at low incidence, reaching a max-

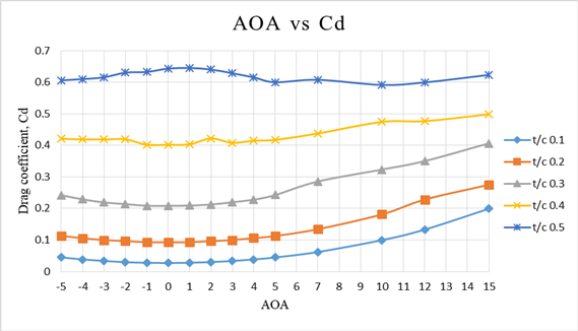


Figure 13: AOA vs drag coeff. at different t/c ratios

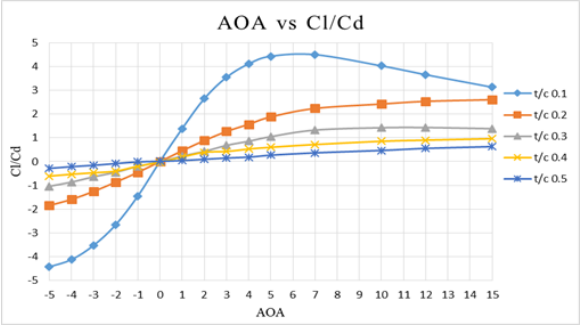


Figure 14: AOA vs Cl/Cd at different t/c ratios

imum at moderate angles of attack before decreasing at higher angles. This behavior reflects the combined influence of quasi-linear lift growth and the increasingly nonlinear rise in drag as angle of attack increases. The location and magnitude of the peak efficiency are strongly dependent on airfoil thickness.

Thinner airfoils consistently achieve higher maximum lift-to-drag ratios compared to thicker configurations. In particular, the t/c = 0.1 and 0.2 airfoils exhibit the highest efficiency values, with peak $\frac{C_l}{C_d}$ occurring at angles of attack in the range of approximately 3°to 5°. In this regime, lift is generated efficiently while wave drag remains relatively low due to weaker shock systems. As thickness increases, both the maximum achievable efficiency and the angle of attack corresponding to peak efficiency decrease. For thicker airfoils (t/c  0.4), the lift-to-drag ratio remains significantly lower across the entire angle-of-attack range. Although these configurations generate slightly higher lift at a given angle of attack, the accompanying increase in drag dominates the efficiency metric, resulting in inferior aerodynamic performance. At higher angles of attack, the rapid growth of wave drag leads to a sharp decline in $\frac{C_l}{C_d}$ for all thickness ratios, with the effect being most pronounced for the thickest airfoils.

These results demonstrate that aerodynamic efficiency at Mach 2 is governed primarily by drag sensitivity rather than lift enhancement. From a design perspective, the findings suggest that relatively thin double-wedge airfoils operated at modest angles of attack offer the most favorable balance between lift generation and drag minimization in supersonic cruise conditions.

### 3.5. Pressure coefficient

The surface pressure characteristics of the double-wedge airfoils are examined through the distribution of pressure coefficient ($C_p$) along the chord for selected thickness ratios at representative angles of attack. Figure XX presents the $C_p$ variation on both the upper and lower surfaces for $\alpha = 0$, highlighting the influence of airfoil thickness under symmetric flow conditions.

For all configurations, a sharp rise in pressure coefficient is observed near the leading edge, corresponding to the compression induced by the oblique shock wave. This pressure jump is more pronounced for thicker airfoils, reflecting the stronger shock generated by the larger effective wedge angle. Immediately downstream of the leading edge, the pressure decreases along the chord due to flow expansion, resulting in a characteristic compression–expansion pattern typical of double-wedge airfoils in supersonic flow.

As thickness increases, the magnitude of the leading-edge pressure coefficient increases substantially, leading to higher stagnation pressures on the windward surface. This behavior directly contributes to the elevated pressure drag observed for thicker airfoils, as discussed in the previous subsections. In contrast, thinner airfoils exhibit lower peak C values and more gradual pressure recovery along the chord, indicating weaker shock strength and reduced wave drag. At the mid-chord location, where the surface inclination changes, a secondary pressure adjustment is evident for all configurations. The intensity of this pressure change increases with thickness, further contributing to pressure losses and drag. Downstream of this region, the pressure gradually recovers toward free-stream levels near the trailing edge.

Overall, the pressure coefficient distributions provide clear physical insight into the aerodynamic performance trends identified in this study. The stronger leading-edge compression and increased pressure gradients associated with thicker airfoils explain their higher drag coefficients and reduced aerodynamic efficiency. Conversely, the smoother pressure variation observed for thinner airfoils supports their superior lift-to-drag performance at Mach 2. These results reinforce the importance of thickness optimization in the aerodynamic design of double-wedge airfoils for supersonic applications.

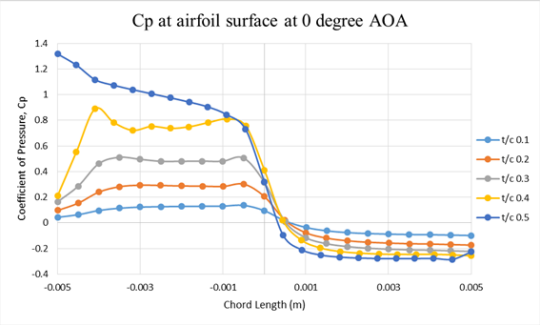


Figure 15: Cp vs Chord length

## 4. Conclusion

A numerical investigation was conducted to evaluate the aerodynamic performance of symmetric double-wedge airfoils at Mach 2 using steady Reynolds–Averaged Navier–Stokes simulations. The effects of thickness-to-chord ratio t/c=0.1–0.5 and angle of attack on lift, drag, aerodynamic efficiency, and surface pressure distribution were systematically analyzed.

The results show that the lift coefficient increases approximately linearly with angle of attack for all configurations, consistent with classical supersonic thin-airfoil theory. Airfoil thickness exerts only a moderate influence on lift, as increased thickness produces slightly larger flow deflection and pressure differences between the upper and lower surfaces.

In contrast, drag is highly sensitive to thickness. As t/c increases, the leading-edge wedge angle becomes larger, generating stronger oblique shocks and higher pressure jumps across the shock. This intensifies entropy generation and total pressure loss, thereby significantly increasing wave drag. The stronger compression also produces steeper chord wise pressure gradients, which further contribute to drag growth. Consequently, drag becomes the dominant factor governing aerodynamic performance in the supersonic regime.

Aerodynamic efficiency, quantified by the lift-to-drag ratio, is maximized for thinner airfoils operating at moderate angles of attack (approximately 3°-5°). The superior performance of thin configurations can be explained by the weaker shock strength associated with smaller wedge angles, resulting in reduced total pressure losses and lower wave drag. At moderate angles of attack, sufficient pressure asymmetry is generated to produce useful lift without excessively strengthening the shock system. However, as the angle of attack increases further, shock intensity and pressure drag rise rapidly, causing a disproportionate increase in drag relative to lift and leading to a marked decline in aerodynamic efficiency. Thicker airfoils exacerbate this effect due to inherently stronger compression waves, resulting in consistently lower lift-to-drag ratios across the entire operating range.

Surface pressure distributions support these observations, showing that higher thickness ratios produce stronger leading-edge compression and larger pressure gradients along the chord. These flow characteristics provide a clear physical explanation for the increased drag penalties and reduced efficiency of thicker configurations.

Overall, the study demonstrates that airfoil thickness is a primary design parameter controlling shock strength, wave drag, and aerodynamic efficiency for double-wedge airfoils at Mach 2. From a supersonic design perspective, relatively thin double-wedge configurations operated at modest angles of attack provide the most favorable compromise between lift generation and drag minimization due to their ability to produce adequate lift while limiting shock-induced total pressure losses.

## References

[1] Anderson J D. History of high-speed flight and its technical development[J/OL]. 2000, 39(5). DOI: 10.2514/3.14800.
[2] Gallego O G, Perez R E, Jansen P W. Technical viability and operational assessment of a supersonic business jet[C/OL]// 2018 Aviation Technology, Integration, and Operations Conference. Atlanta, Georgia: American Institute of Aeronautics and Astronautics, 2018. DOI: 10.2514/6.2018-3661.
[3] Kabir A, Hossain S M, Hafiz A, et al. Aerodynamic analysis on double wedge airfoil at different mach numbers with varying angle of attacks using computational fluid dynamics[C/OL]// 2019 International Conference on Computer, Communication, Chemical, Materials and Electronic Engineering (IC4ME2). IEEE, 2019: 1-6. DOI: 10.1109/IC4ME247184.2019.9036555.
[4] Vincenti W G, Dugan D W, Phelps E. An experimental study of the lift and pressure distribution on a double-wedge profile at mach numbers near shock attachment[R/OL]. 1954. https://ntrs.nasa.gov/api/citations/19930084152/downloads/19930084152.pdf.
[5] Hasan M M, Rahaman M M, Zakaria N M G. Fast aerodynamics prediction of wedge tail airfoils using multi-head perceptron network[J/OL]. Arabian Journal for Science and Engineering, 2024, 49(8): 11397-11423. DOI: 10.1007/s13369-023-08686-9.
[6] Pittman J L. Supersonic airfoil optimization[J/OL]. Journal of Aircraft, 1987, 24(12): 873-879. DOI: 10.2514/3.45532.
[7] Rashid S, Nawaz F, Maqsood A, et al. Review of wave drag reduction techniques: Advances in active, passive, and hybrid flow control[J/OL]. Proceedings of the Institution of Mechanical Engineers, Part G: Journal of Aerospace Engineering, 2022. DOI: 10.1177/09544100211069796.
[8] Lagerstrom P A, Graham M E. Linearized theory of supersonic control surfaces[J/OL]. 2012. DOI: 10.2514/8.11719.
[9] Kaushik M. Potential flow theory[M/OL]// Kaushik M. Theoretical and Experimental Aerodynamics. Singapore: Springer, 2019: 107-126. DOI: 10.1007/978-981-13-1678-4_4.
[10] Vos R, Farokhi S. Shock-expansion theory[M/OL]// 2015. DOI: 10.1007/978-94-017-9747-4_4.

[11] Zulkarna-En M, Islam M A, Al-Faruk A, et al. Numerical analysis of aerodynamic and shock wave characteristics of biconvex and double-wedge shape airfoils for supersonic flow[J]. International Journal of Automotive and Mechanical Engineering, 2023, 20(4): 10821-10837.

[12] Kesler S R, Hunsaker D F. Aerodynamic centers of symmetric diamond airfoils in inviscid supersonic flow[C/OL]// AIAA SCITECH 2026 Forum. American Institute of Aeronautics and Astronautics, 2026. DOI: 10.2514/6.2026-1330.

[13] Vijayaparkavan P, Lewise A S, Raj R A. A review on 2-d supersonic aerofoil shape optimization[J/OL]. Computational Mathematics and Mathematical Physics, 2024. DOI: 10.1134/S0965542524701586.

[14] Golmirzaee N, Wood D H. Some effects of domain size and boundary conditions on the accuracy of airfoil simulations[J/OL]. Advances in Aerodynamics, 2024, 6(1): 7. DOI: 10.1186/s42774-023-00163-z.

[15] Prasad U S, Ajay V S, Rajat R H, et al. Aerodynamic analysis over double wedge airfoil[J/OL]. IOP Conference Series: Materials Science and Engineering, 2017, 197(1). DOI: 10.1088/1757-899X/197/1/012076.

[16] Arnold J H. Vapor viscosities and the sutherland equation[J/OL]. Journal of Chemical Physics, 1933, 1(2): 170. DOI: 10.1063/1.1749269.

[17] Tandra D S, Kaliazine A, Cormack D E, et al. Numerical simulation of supersonic jet flow using a modified k-epsilon model[J/OL]. International Journal of Computational Fluid Dynamics, 2006, 20(1): 19-27. DOI: 10.1080/10618560600587204.

[18] Dhungana B, Bhattrai S, Paudel S. Aeroelastic analysis of a suav half span wing within pre-stall region using a two-way closely coupled fsi model[J/OL]. Journal of The Institution of Engineers (India): Series C, 2026. DOI: 10.1007/s40032-026-01320-1.

[19] Mahony J J. A critique of shock-expansion theory[J/OL]. Journal of the Aeronautical Sciences, 1955, 22(10): 673-680. DOI: 10.2514/8.3433.

[20] Lagerstrom P A, Graham M E. Linearized theory of supersonic control surfaces[J/OL]. Journal of the Aeronautical Sciences, 1949, 16(1): 31-34. DOI: 10.2514/8.11719.